Supporting Information

Materials and Methods

Sample preparation and data-acquisition:

Unless otherwise noted, interference samples were prepared as previously described[1]. HeLa S3 cells were grown in suspension to $1x10^6$ cells/mL. Yeast cells were grown to an OD of 1.0. Cells were lysed in 6 M guanidinium thiocyanate, 50 mM Hepes pH 8.5 (HCl). Protein content was measured using a BCA assay (Thermo Scientific), disulfide bonds were reduced with dithiothreitol (DTT), and cysteine residues alkylated with iodoacetamide as previously described [2]. Protein lysates were cleaned up by methanol-chloroform precipitation[3]. The samples were taken up in in 6 M guanidium thiocyanate, 50 mM Hepes pH 8.5, and diluted to 1.5 M guanidium thiocyanate, 50 mM Hepes, pH 8.5. Both lysates were digested over night with Lys-C (Wako) in a 1: 50 enzyme: protein ratio digest. Following digestion, the sample was acidified with tri-fluoric-acid to a pH < 2, and subjected to C_{18} solid-phase extraction (SPE) (Sep-Pak, Waters). Amino reactive TMT reagents (126 to 131, Thermo Scientific, Lot # MJ164415, 0.8 mg) were dissolved in 40 µl acetonitrile, and 10 µl of the solution was added to 100 µg of peptides dissolved in 100 µl of 50 mM HEPES (pH 8.5). After 1 h at room temperature (22 °C), the reaction was quenched by adding 8 µl of 5% hydroxylamine. Following labeling, the sample was combined in desired ratios (e.g., 1: 4: 10: 4: 1). A fraction of the labeled yeast sample was kept separately from the labeled human sample, and that sample was prepared for interference free analysis. Samples were subjected to C_{18} solid-phase extraction (SPE) (Sep-Pak, Waters).

LC-MS experiments were performed on an Orbitrap Elite or QEactive MS (Thermo Fischer Scientific). The Orbitrap Elite was equipped with a Famos autosampler (LC Packings) and an Agilent 1100 binary high-pressure liquid chromatography (HPLC) pump (Agilent Technologies). For each run ~1µg of peptides were separated on a 100 or 75 µm inner diameter microcapillary column packed first with

approximately 0.5 cm of Magic C_4 resin (5 µm, 200 Å, Michrom Bioresources) followed by 20 cm of Maccel C_{18} AQ resin (3 µm, 200 Å, Nest Group). Separation was achieved by applying a 9–32% acetonitrile gradient in 0.125% formic acid over 90 min at ~ 300 nl/min. Electrospray ionization was enabled through applying a voltage of 1.8 kV through a PEEK micro-tee at the inlet of the microcapillary column. The Orbitrap Elite was operated in data-dependent mode. The survey scan was performed in the Orbitrap over the range of 300–1,500 *m/z* at a resolution of 84 k, followed by the selection of the ten most intense ions (top 10) for HCD-MS2 fragmentation using a precursor isolation width window of ±2 *m/z* followed by MS2 with a resolution of a resolution of 42 k. The automatic gain control (AGC) settings were 3×10^6 ions and 5×10^5 ions for survey and MS2 scans, respectively. Ions were selected for MS2 when their intensity reached a threshold of 500 counts and an isotopic envelope was assigned. Maximum ion accumulation times were set to 1,000 ms for survey MS scans and to 250 ms for MS2 scans. The normalized collision energy for HCD-MS2 experiments was set to 32% at a 30-ms activation time. Singly-charged and ions for which a charge state could not be determined were not subjected to MS2. Ions within a ±10 ppm *m/z* window around ions selected for MS2 were excluded from further analysis for 120 s.

The QExactive was equipped with easy-nLC 1000 UHPLC pump. For each run ~1µg of peptides were separated on a 75 µm inner diameter microcapillary column packed first with approximately 0.5 cm of Magic C_4 resin (5 µm, 200 Å, Michrom Bioresources) followed by 25 cm of GP-C18 resin (1.8 µm, 120 Å, Sepax Technoligies). Separation was achieved by applying a 9–32% acetonitrile gradient in 0.125% formic acid over 90 min at ~400 nL/min. Electrospray ionization was enabled through applying a voltage of 1.8 kV through a PEEK junction at the inlet of the micro capillary column. The QExative was operated in data-dependent mode. The survey scan was performed at a resolution setting of 70 k, followed by the selection of the ten most intense ions (top 10) for HCD-MS2 fragmentation. The normalized collision energy for HCD-MS2 experiments was set to 30%. Singly-charged and ions for which a charge state could not be determined were not subjected to MS2. Ions for MS2 were excluded from further selection

for fragmentation for 40 s. For a test of different parameters for TMT^C quantification on a QExactive see supplementary figure 6. We optimized the collision energy settings and we obtain the best numbers with the configurations used throughout this study (data not shown). Raw data are available upon request through our high-speed transfer server.

Data analysis

A suite of in-house-developed software tools was used to convert mass spectrometric data from the RAW file to the mzXML format, as well as to correct erroneous assignments of peptide ion charge state and monoisotopic *m/z*[4]. We modified the ReAdW.exe to include signal to noise ratios (S/N) for each peak during conversion to the mzXML file format (http://sashimi.svn.sourceforge.net/viewvc/sashimi/). Assignment of MS2 spectra was performed using the Sequest algorithm[5] by searching the data against a protein sequence database including all entries from the human International Protein Index database (version 3.6) followed by sequences of proteins encoded by all known *S. cerevisiae* ORFs, and known contaminants such as human keratines. This forward (target) database component was followed by a decoy component including all listed protein sequences in reversed order. Protein sequences from the human database were listed before those from yeast so that a peptide included in both databases was always assigned to a human protein and did not intervene with measuring the interference effect. Searches were performed using a 20 ppm precursor ion tolerance, where both peptide termini were required to be consistent with Lys-C specificity, while allowing up to two missed cleavages. TMT tags on lysine residues and peptide N termini (+ 229.162932 Da) and carbamidomethylation of cysteine residues (+57.02146 Da) were set as static modifications, oxidation of methionine residues (+ 15.99492 Da) as a variable modification. An MS2 spectral assignment false discovery rate of less than 1% was achieved by applying the target-decoy database search strategy[6]. Filtering was performed using a linear discrimination analysis method to create one combined filter parameter from the following peptide ion and MS2 spectra properties: Sequest parameters XCorr and ΔCn, absolute peptide ion mass accuracy and charge state.

Forward peptides within 3 standard deviation of the theoretical *m/z* of the precursor were used as positive training set. All reverse peptides were used as negative training set. Linear discrimination scores were used to sort peptides with at least 6 residues and to filter with a cutoff of 1% false discovery rate based on the decoy database[4].

Each search was software-recalibrated to alleviate any systematic mass error dependent on peptide elution time or observed *m/z*. All ions in the full MS1 spectra were first adjusted. A representative subset of peptides was selected using those above the median XCorr and within one standard deviation of the global mass error. The mass errors of this subset were then fit to each parameter using LOESS regression. The *m/z* of every ion in MS1 spectra was then adjusted by the error predicted by interpolating the values of the nearest data points in the regression model. Adjustments for each of the two parameters were done iteratively. MS2 spectra were then calibrated in a similar manner. Mass errors were calculated from matched peptide fragment ions within two standard deviations of the global mass error and above the upper quartile of intensity. Mass errors were fitted to each parameter using LOESS regression and the *m/z* for every ion in MS2 spectra was adjusted as above.

For quantification via the reporter ions the intensity of the signal closest to the theoretical *m/z,* within a ±20 ppm window, was recorded. Reporter ion intensities were adjusted based on the overlap of isotopic envelopes of all reporter ions as recommended by the manufacturer.

The peak that resulted from the monoisotopic-precursor labeled with the most abundant peak of TMT-131, after fractionation, was defined as Position 0. Peak intensity (S/N) from Position -1 to +10 were extracted for quantification. The peak closest to the predicted mass was chosen within a ± 20 ppm. window. We calculated the theoretical mass difference from the pseudo monoisotopic mass minus or plus the mass-difference between C13 and C12 (1.00336 Da).

For figure 5 the dta file was manually edited to represent two peptides based on charge state and *m/z* values of the surviving precursor in the MS2 spectrum. This dta file was searched against the yeast human-peptide database (including decoy) with 5 ppm window.

Deconvolution of TMT^C ion cluster with theoretical precursor envelope

To measure the TMT isotopic impurities of the TMT-reagents we combined each amino-reactive-TMT separately with ammonium carbonate and measured the isotopic envelope from the resulting TMT-NH_2 in the MS1 (We neglected the NH_2 isotopic envelope, which is ~ 0.4% for the +1 peak when the entire envelop is normalized to 1). We observed an isotopic envelope made up of three peaks at ~246, 247 and 248 m/z with abundance of > 1% when the entire envelope is normalized to 1. From these isotopic envelopes we selected each peak individually, fragmented it with HCD, and measured the resulting reporter ions (~126 Da to ~132 Da). From these spectra, we derive six TMT-impurity matrices $\boldsymbol{I_{126}}$... $\boldsymbol{I_{131}}$, which are graphically represented in supplementary figure 2. Each entry reports the relative abundance of isotopes and their fragmentation pattern (the matrices are normalized to 1). The columns define the position in the TMT-NH2 precursor isotopic envelope (~246, 247, 248 Da left to right) while rows from top to bottom corresponds to the delta mass (Δ m) which is the mass difference between this precursor ion and its resulting TMT^C ion after fragmentation (~154 Da to ~159 Da, top to bottom). The six different delta masses arise from 5 different TMT channels (126 to 131, without 129 as we cannot distinguish the delta mass of 129 and 130; Suppl. Fig. 1) and an additional ion at ~132 Da, which is the result of an isotopic impurity in the 131-TMT tag.

$$I_{126} = \begin{bmatrix} 0.032 & 0.875 & 0.047 \\ 0.000 & 0.014 & 0.032 \\ 0.000 & 0.000 & 0.000 \\ 0.000 & 0.000 & 0.000 \\ 0.000 & 0.000 & 0.000 \\ 0.000 & 0.000 & 0.000 \end{bmatrix} I_{127} = \begin{bmatrix} 0.004 & 0.000 & 0.000 \\ 0.036 & 0.880 & 0.040 \\ 0.000 & 0.004 & 0.036 \\ 0.000 & 0.000 & 0.000 \\ 0.000 & 0.000 & 0.000 \\ 0.000 & 0.000 & 0.000 \end{bmatrix}$$

$$I_{128} = \begin{bmatrix} 0.000 & 0.000 & 0.000 \\ 0.010 & 0.000 & 0.000 \\ 0.018 & 0.896 & 0.051 \\ 0.000 & 0.000 & 0.026 \\ 0.000 & 0.000 & 0.000 \\ 0.000 & 0.000 & 0.000 \end{bmatrix} I_{129} = \begin{bmatrix} 0.000 & 0.000 & 0.000 \\ 0.000 & 0.000 & 0.000 \\ 0.029 & 0.000 & 0.000 \\ 0.021 & 0.900 & 0.073 \\ 0.000 & 0.000 & 0.000 \\ 0.000 & 0.000 & 0.000 \end{bmatrix}$$

$$I_{130} = \begin{bmatrix} 0.000 & 0.000 & 0.000 \\ 0.000 & 0.000 & 0.000 \\ 0.001 & 0.000 & 0.000 \\ 0.021 & 0.906 & 0.065 \\ 0.000 & 0.000 & 0.008 \\ 0.000 & 0.000 & 0.000 \end{bmatrix} I_{131} = \begin{bmatrix} 0.000 & 0.000 & 0.000 \\ 0.000 & 0.000 & 0.000 \\ 0.000 & 0.000 & 0.000 \\ 0.026 & 0.000 & 0.000 \\ 0.000 & 0.900 & 0.062 \\ 0.000 & 0.000 & 0.012 \end{bmatrix}$$

For each of the TMT channels we can also define the vector of isotopic impurities $t_{126}…t_{131}$ by summing the rows of the respective matrices $I_{126}…I_{131}$. That is, the isotopic impurity vector $t_{126} = [0.032 \quad 0.889 \quad 0.079]$ where the numbers represent the relative abundance, regardless of fragmentation pattern, of the TMT-NH2 ions with ~246, 247 and 248 Da respectively.

The vector $\boldsymbol{p}$ represents the relative population of the isotopic envelope for a given non-TMT-labeled peptide. This vector can be calculated from the amino acid composition based on the natural abundance of isotopes [7]. The first position in this vector $p(0)$ is the position of the monoisotopic peak. The following positions are the peaks which are one mass unit (~1.003 Da) heavier. The values in $\boldsymbol{p}$ are normalized to 1.

The number of TMT-tags ($\boldsymbol{k}$) bound to a peptide is the number of lysine-residues +1 (N-terminus). From $\boldsymbol{I}$, $\boldsymbol{t}$, $\boldsymbol{k}$ and $\boldsymbol{p}$ we can calculate the precursor matrix $\boldsymbol{P_{TMT}}$ (See also Suppl. Fig. 3).

$$for\ \boldsymbol{TMT = 126 \ldots 131} \qquad \boldsymbol{P_{TMT} = I_{TMT} * p *^{k-1} t_{TMT}}$$

In these matrices $\boldsymbol{P_{TMT}}$ the rows indicate the delta mass after fragmentation as described for $\boldsymbol{I_{TMT}}$ and the columns indicate the position in the isotopic envelope. We calculate columns p(-1) to p(10), with the pseudo-monoisotopic peak defining position p(0).

For given mixing ratios r_{TMT} (expressed as r_{126}: r_{127}: r_{128}: r_{130}: r_{131}, normalized to 1) we can calculate the distribution of delta masses throughout the isotopic precursor envelope encoded in the Precursor -Matrix P_M, which is calculated as a weighted sum of the $P_{126} \ldots P_{131}$ matrices:

$$P_M = \sum_{i=126 \ldots 131} r_i P_i$$

From this matrix P_M we can calculate the relative abundance of ions in the theoretical TMT^C ion cluster which we represent with the vector $\hat{c}$. The position $\hat{c}(0)$ is defined as the position which results from loss of the TMT-131 reporter ion of the pseudo moniosotopic peak $p(0)$. We calculate $\hat{c}$ for positions -1 to 14.

$$\hat{c}_k = \sum_{i,j} P_{M_{i,j}}$$

$$\text{with } i + k - 5 = j, \qquad k = -1 \ldots 14, \qquad i = 1 \ldots 6, \qquad j = -1 \ldots 10$$

This is equivalent of summing up the diagonals of P_M.

Next we compare theoretically calculated vector $\hat{c}$ for the TMT^C ion cluster with the observed ion cluster c. To avoid fitting noise of empty positions we first calculate which positions in the theoretically predicted TMT^C envelope $\hat{c}$ are populated with less than 1% of the total ion cluster for the theoretical ratios $\hat{r}_{TMT} = 0.2 : 0.2 : 0.2 : 0.2 : 0.2$. For typical peptides this requirement is fulfilled for the pseudo-monoistopic position $\hat{c}(0)$ to $\hat{c}(+6)$ to $\hat{c}(+8)$. We than vary the ratio in r_{TMT} and minimize $Diff$[8].

$min_{\hat{r}}\, Diff\left(c, \hat{c}(\hat{r})\right) = min_{\hat{r}} \sum_i (\hat{c}_i(\hat{r}) - c_i)^2$ for all i where $\hat{c}_i(\hat{r}_{TMT}$=0.2:0.2:0.2:0.2:0.2) > 0.01 with $\sum_i \hat{c}_i = 1$ and $\sum_i c_i = 1$

Searching for the mixing proportions which minimize the ion envelop similarity function is a standard multi-variate optimization problem. $Diff$ is defined as quadratic similarity function. We therefore obtain

an instance of convex optimization and can solve the optimization problem with a simple local search solver as implemented by the fmincon function in MATLAB.

To filter for well quantified peptides we require at least ~1000 ions in the TMT^C envelope and a ***minDiff*** value of <0.005. For the purposes of this paper, we focus on individually solving this for each peptide, while an obvious extension of this method would be to solve jointly for all peptides of a given protein.

The MS3 method was performed as previously described[1], on an Orbitrap Elite. For successful quantification, we required at least 500 reporter ions, which has become the standard used in our lab.

Estimation of number of ions in peak

For spectra acquired in an Orbitrap we assume that the number of ions in a peak is proportional to signal-to-noise over charges. We estimate the number of molecules in a given fragment ion peak using the assumption that the noiseband is approximately equal to 5 charges when the transient is 30 ms long and collected on a D20 Orbitrap. This number was estimated based on a comparison of charges in the orbitrap with the ion-trap on the Orbitrap Elite. This correlates well with previous published results[9]. The D20 Orbitrap in the Elite aquires the same signal-to-noise for a given number of same ions in half the time when compared to the D30 Orbitrap in the QExactive[10]. For differing resolutions (longer acquisition times) noise decreases with the square root of acquisition time[9] while signal stays approximately constant. As a result we assume that the noiseband of a MS2-spectrum on the QExactive is equivalent to charges (e) as follows: 5 e at 18k nominal resolution, 3.5 e at 35k, and 2.5 e at 70k. Analogously, the noiseband for the Orbitrap Elite is estimated to be 5 e at 21k, and 3.5 e at 42k (All nominal resolution are expressed for 200 *m/z*).

Supplementary Figures

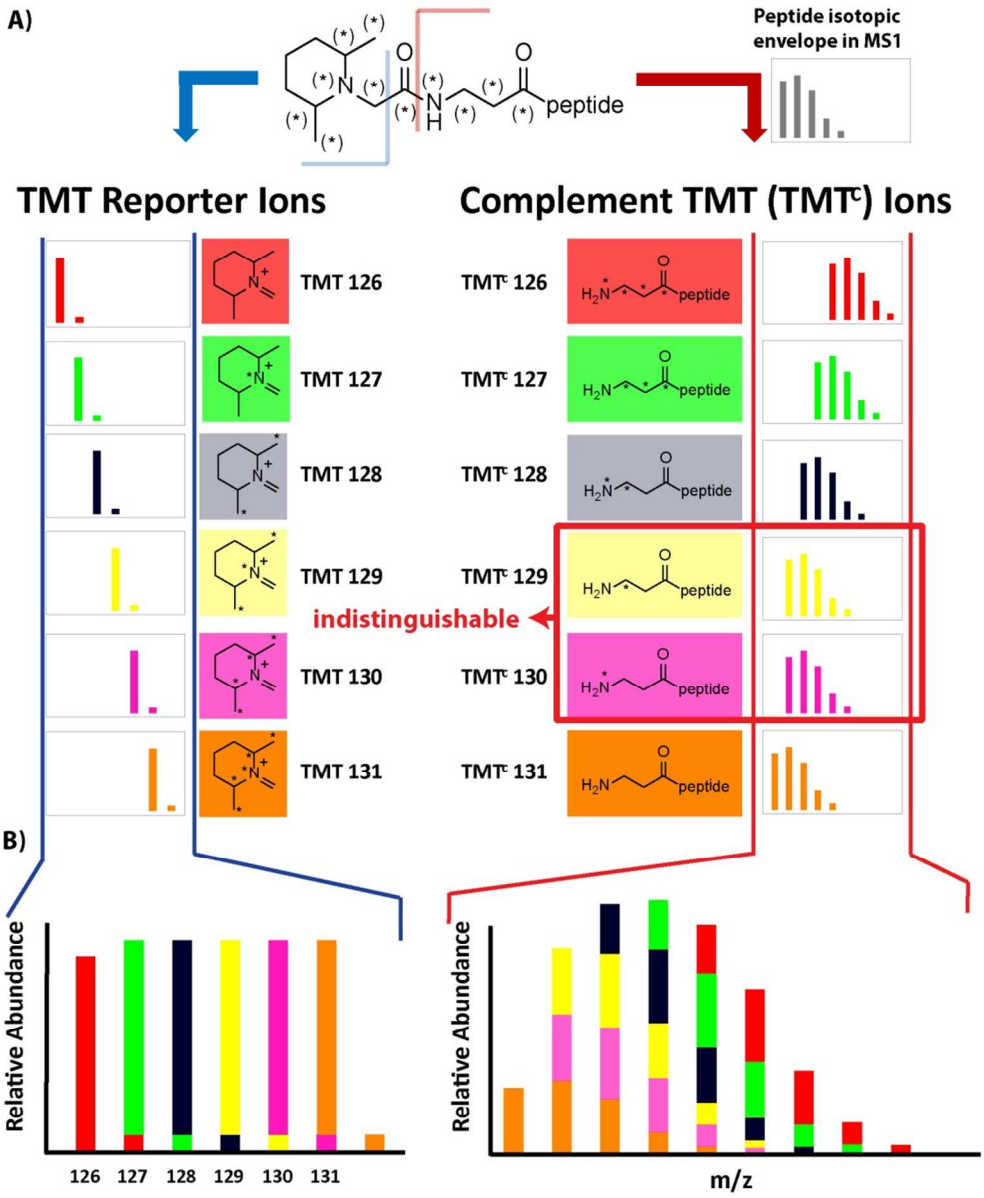

Suppl. Fig. 1: Formation of TMT reporter ions and TMT^C ion cluster. A) Fragmentation of a six-plex TMT-labeled peptide. Asterisks indicate sites of heavy isotopes (^{13}C or ^{15}N). TMT reporter ions and TMT^C ions are formed through bond cleavage at the indicated positions. The *m/z* of both reporter ions and TMT^C ions are channel specific. However, the MS2 mass resolution setting used in this study was not sufficient to resolve TMT^C-129 and TMT^C-130 ions and the TMT-129 channel was therefore not used. **B)** Peptide quantification is rather uncomplicated using the low *m/z* TMT reporter ions, but challenging for the TMT^C ion cluster which results from the overlap of the

high *m/z* TMT^C ion envelopes of each individual TMT channel. Peptides are quantified by deconvolving the TMT^C cluster using our knowledge of the theoretical ion intensity distribution of the isotopic envelope of the precursor peptide.

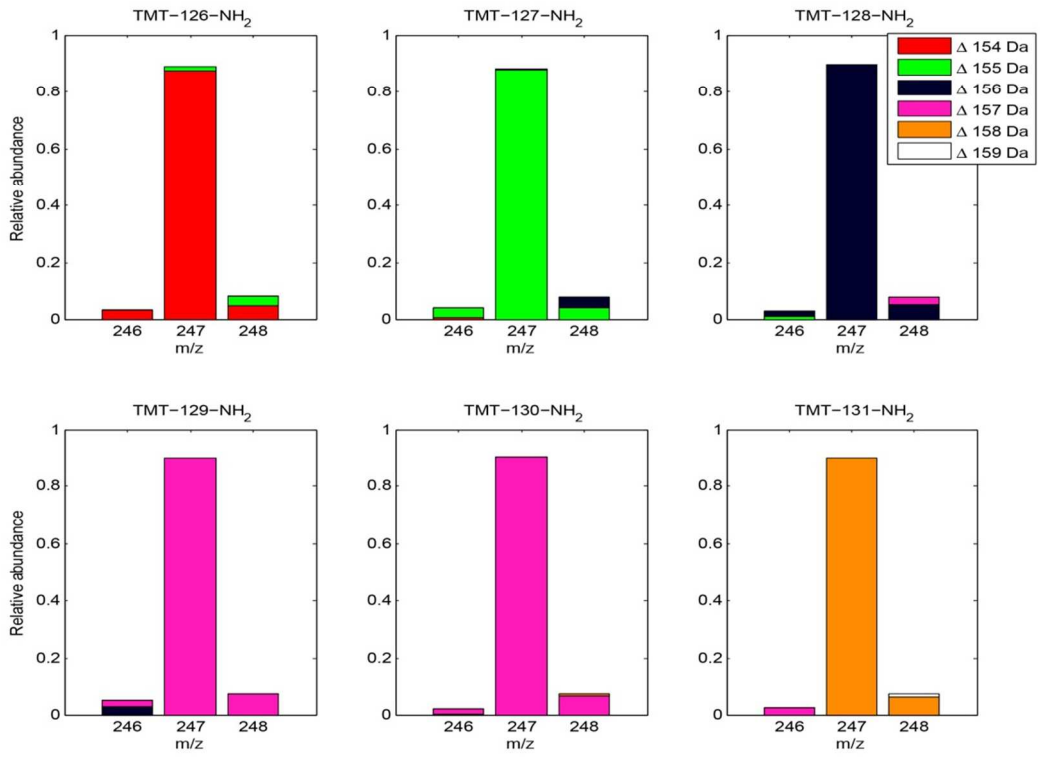

Suppl. Fig. 2: Determining the exact isotopic composition of TMT tags. The six different amino reactive TMT-tags were reacted with ammonium bicarbonate. The intensity distributions of the resulting NH_2-TMT isotopic envelopes were individually measured on an Orbitrap Elite mass spectrometer. The *m/z* of the pseudo-monoisotopic is set to 247. Next each individual precursor peak was fragmented in an individual MS2 experiment, and its contribution to the intensity of each individual reporter ion was determined. These measurements allowed us to infer the generation of the TMT^C ions (color coded). The six listed mass decrement values arise from the use of 5 different TMT reagents [126, 127, 128, 130, and 131 (Suppl. Fig. 1)] and the consideration of an additional ion at 132 *m/z* resulting from an isotopic impurity in the TMT-131 reagent.

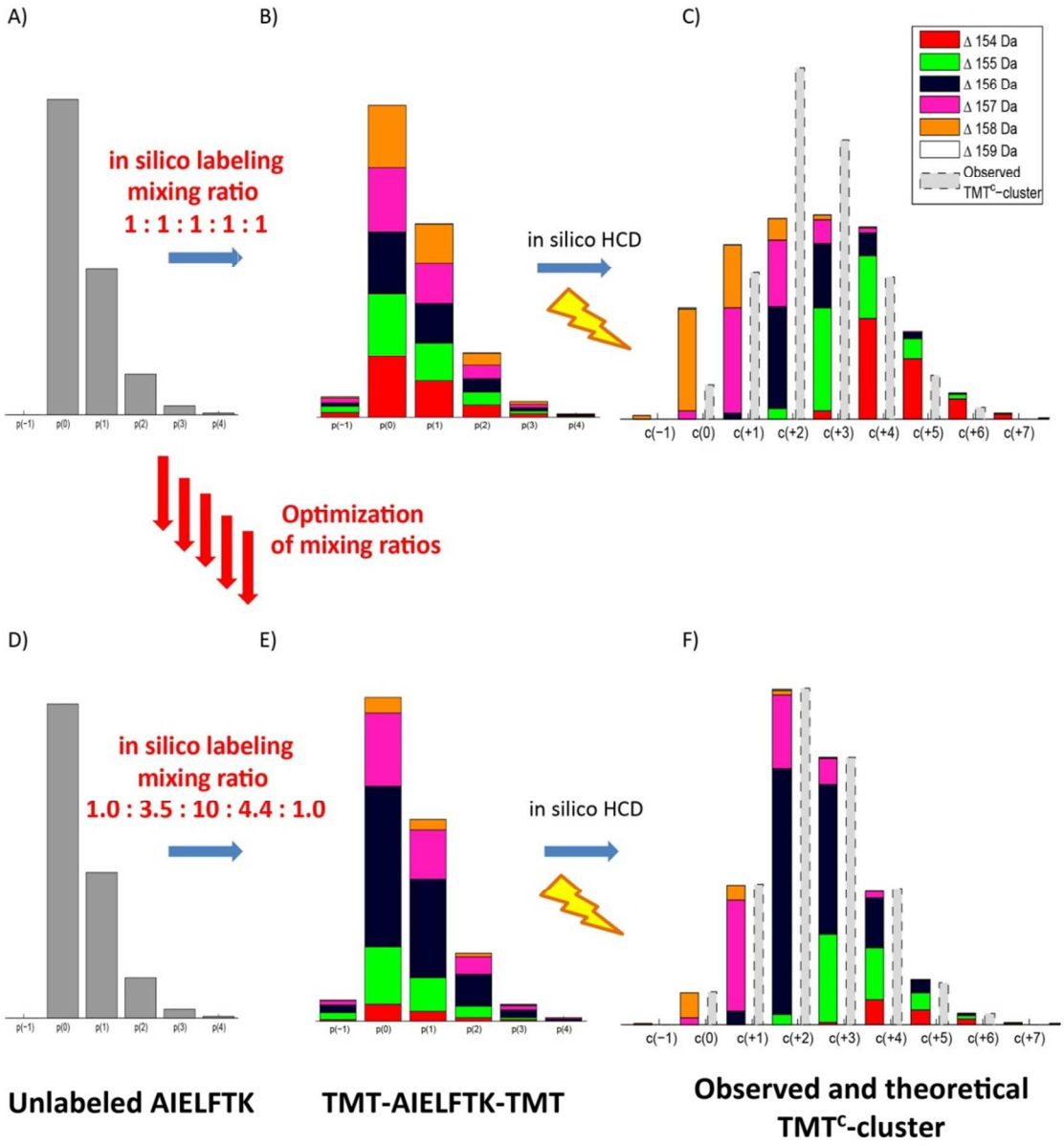

Suppl. Fig. 3: TMT^C ion cluster-based quantification using the example of the yeast peptide AIELFTK from the human-yeast interference sample (see also Fig. 2). A) Predicted relative intensity distribution in the isotopic envelope for the unlabeled peptide. The monoisotopic peak is positioned at p(0). **B)** The isotopic envelope and the intensity distribution for mass decrement ions are calculated for a peptide with two TMT-tags (one at the N-terminus, one at the lysine-residue) for an arbitrarily chosen mixing ratio of 1:1:1:1:1. The mass decrements indicate the mass difference between the *m/z* value of an ion in the isotopic envelope of the precursor ion and its *m/z* value in the TMT^C cluster. By approximation, a mass decrement of 154 Da is equivalent to TMT-126, a decrement

of 155 Da is equivalent to TMT-127, and so forth (a detailed annotation of mass decrements to TMT-channels is given in Suppl. Fig. 2 and in matrix form in Materials and Methods). Due to the distribution of isotopic impurities in the TMT-tag, the relative abundance of the different mass-decrements throughout the precursor envelope are not constant (e.g. the p(-1) position is nearly free of the 158 Dalton decrement) **C)** We are able to calculate the intensity distribution of the theoretical TMT^C envelope based on the distribution of mass decrements in the precursor ion cluster. The predicted intensity distribution in the TMT^C ion cluster is compared with the observed values (grey). D, E, F) According to A-C, the predicted contributions of each TMT channel are optimized so that the summed square difference between observed and predicted TMT^C cluster intensity is minimal. For the shown example the optimized predicted ratios for the TMT channels 126: 127: 128: 130: 131 are 1.0: 3.5: 10: 4.4: 1.0.

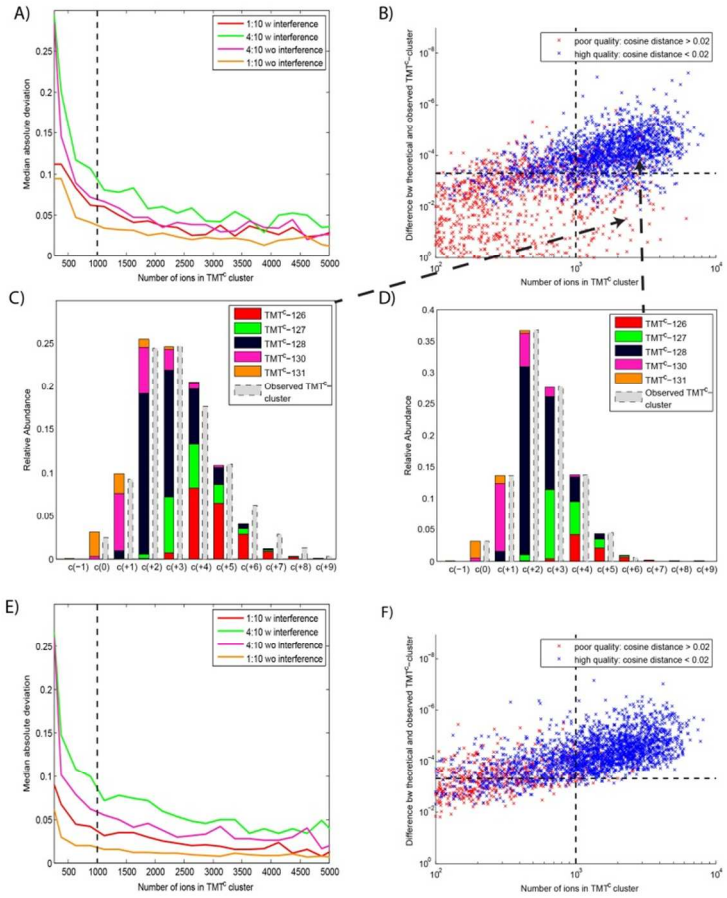

Suppl. Figure 4: Filtering of TMT^C-based quantitative data. A) Relative yeast peptide TMT channel intensities were calculated by de-convolving the TMT^C ion cluster. The graphs show the median absolute deviation of the measured ratios from the expected 1:10 and 1:4 ratios plotted against the number of ions in the TMT^C envelope. Measurements were taken in absence and under the influence of interference by human peptides. We decided to use a cutoff of 1000 ions as a minimum requirement for confident quantification. **B)** As a second filter criterion we used the summed square difference (Diff) between predicted and observed TMT^C ion cluster. We defined peptides with a cosine distance of less than 0.02 between measured and predicted TMT channel ratios as well quantified peptides. The graph shows well-quantified peptides (blue) and other peptides (red) for their sum of ions in TMT^C cluster and the sum of

squared difference between observed and calculated TMT^C cluster. The dotted black lines indicate the filtering thresholds used throughout this study. **C)** Predicted and observed TMT^C isotopic cluster for a peptide which did not meet the filter criteria (Diff = 0.0017). **D)** An example where predicted and observed TMT^C isotopic cluster agree well (Diff = 0.0002). **E)** Similar to the graph shown in A, this plot shows data for Monte Carlo simulated yeast peptides with known mixing ratios based on amino-acid sequence and number of ions observed in experiment described in A,B. Data from the simulated and actual experiment are very similar. **F)** Data from a Monte Carlo simulated experiment plotted as described in B. The distribution of most data-points is very similar between simulated and actual experiment. However, the actual experiment produced more outliers, which are likely due to occasional interference of the measured TMT^C envelope through contaminating ions.

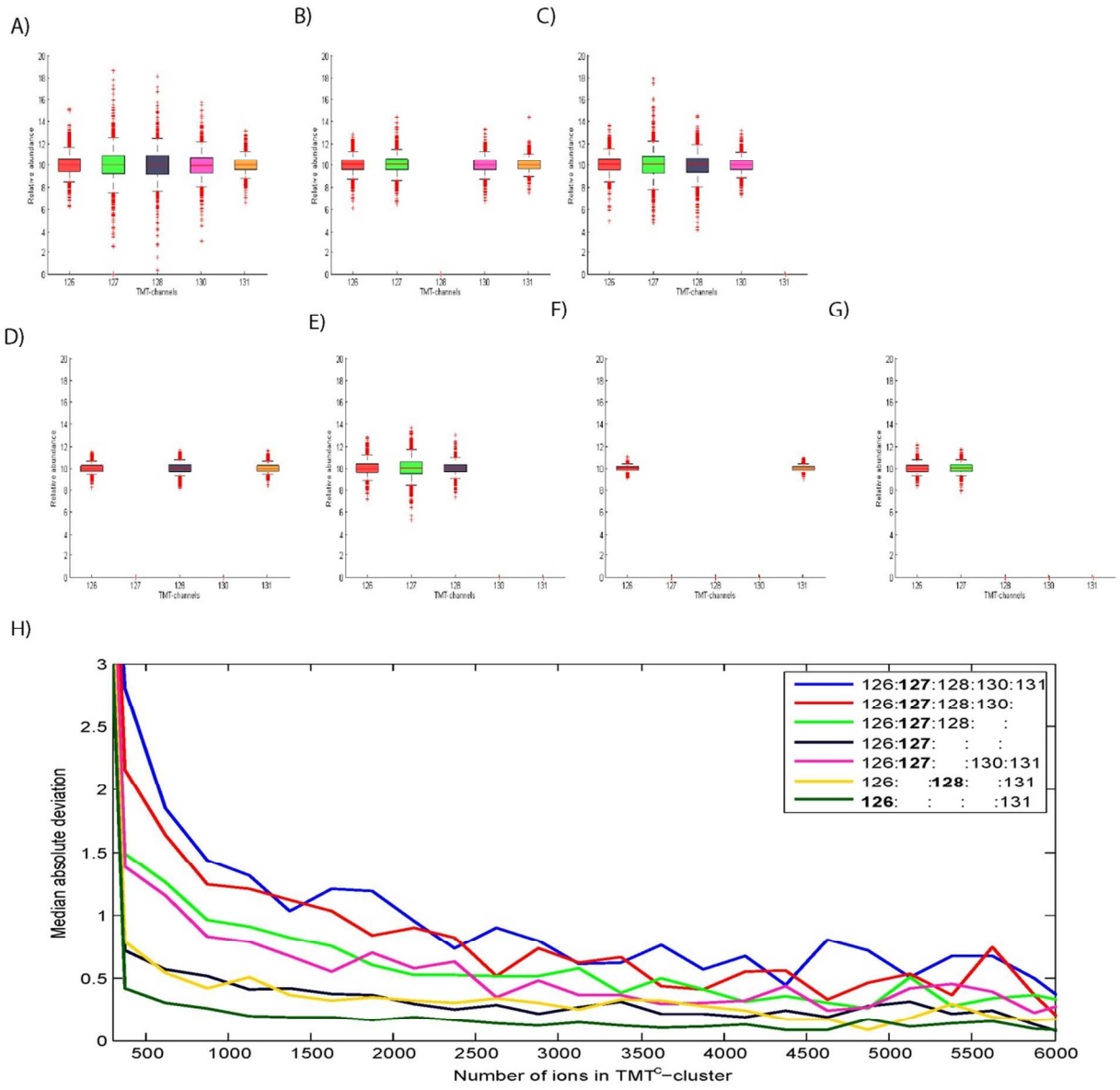

Suppl. Fig. 5: Evaluation of the influence of channel number and inter-channel mass spacing on precision of TMT^C-based peptide quantification. A simulation of an experiment with TMT channels mixed in equal amounts was performed based on the amino-acid-sequences and number of ions observed in the experiment shown in figure 3A, B. Panels A-G depicts boxplots from these experiments with the sum of the ratios normalized to the number of channels multiplied by 10. Only data from TMT^C ion clusters with at least 1000 ions were considered. Whiskers reach from the 5 to 95 percentile. **A)**

Simulation for the use of all five-plex TMT as applied throughout this study. **B)** Removing the 128 channel notably increases the precision of the quantitative data. **C)** Data for using 4 channels without inter-channel mass-spacing. Almost no increase of quantitative precision is shown in comparions to the data from using all five channels as presented in B. **D,E)** Simulated 3-plex experiment with (D) and in the absence (E) of mass- spacing between channels. As expected, the precision is substantially higher in E as the deconvolution of the TMT^C cluster is less complicated. **F,G)** Comparison of duplex sample with and without mass-spacing. **H)** Values for the median absolute deviation are plotted versus the total number of ions in TMT^C cluster for experiments with varying numbers of channels and with and without mass-spacing between the channels (corresponding to the experiments shown in A-G). For each experiment the channel with the poorest precision was selected for the plot (bold in legend). While the precision improves with increasing number of ions for all experiments, approximately ten-times more ions are required for the 5-plex sample to obtain a precision similar to that achieved in the experiment using 3 channels separated by 2 Da mass-spacing.

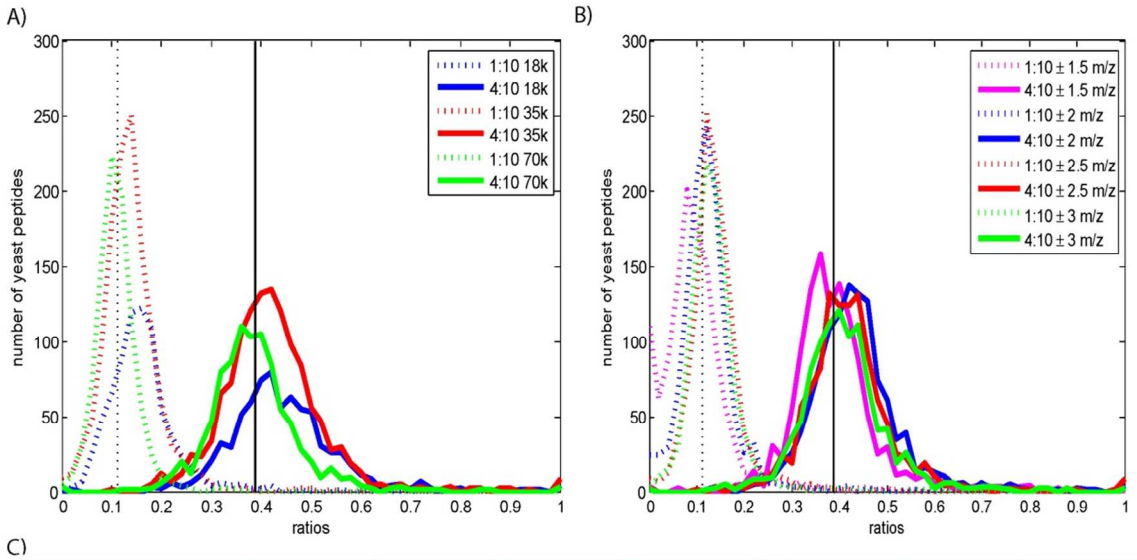

C)

	±1.5 m/z, 35k, 240ms inj-time	±2 m/z, 35k, 240ms inj-time	±2.5 m/z, 35k, 240ms inj-time	±3 m/z, 35k, 240ms inj-time		±2mz, 18k, 60ms inj-time	±2mz, 35k, 120ms inj-time	±2mz, 70k, 240ms inj-time
Acquired MS2 spectra	13118	13384	13555	13524		33087	22024	11109
Identified peptides (FDR 1%)	6266	6071	5902	3981		13640	9390	4514
Identified yeast peptides	2850	2775	2717	2699		5612	4029	2140
>1000 ions in TMT^C cluster	1375	1389	1332	1243		1138	1567	982
After "Goodness of Fit" filter	1185	1185	1118	1037		757	1291	912

Suppl. Fig 6: Method optimization for TMT^C-based quantification using the QExactive. A) Comparison of different MS2 resolution settings: for 18 k, 35 k, and 70 k; nominal at 200 *m/z*. Maximum ion injection times were set in accordance with Orbitrap scan times at different resolution settings: 60 ms, 120 ms, and 240 ms, respectively. Vertical lines indicate the known mixing ratios of 1:10 (dotted) and 4:10 (solid). Even at a resolution setting of 18 k systematic error due to interference seems minor. However, the comparatively short ion injection time associated with the 18 k resolution setting – and, consequently, the low number of accumulated ions - led to an increase of TMT^C ion clusters that did not fulfill the data filtering criteria described in Suppl. Fig. 4. At 35 k resolution most peptides passed the filtering criteria;a narrower ratio distribution show that the used settings increased the precision of the acquired quantitative data. **B)** Comparison of different isolation width settings and the effect on TMT^C ion-based quantification at 35 k resolution. An incomplete isolation of the precursor ion envelope when

applying an isolation width of ±1.5 *m/z* (pink) strongly affected the accuracy of the quantitative results. This problem was solved by extending the isolation width to ±2 *m/z*. A further extension of the isolation width to ±2.5 and ±3 *m/z*, respectively, did not significantly improve the accuracy of quantification but decreased the number of identified peptides. We believe that the latter can be attributed to the increased co-isolation of contaminating peptide ions. **C)** Numbers of MS2 spectra, identified, and quantified peptides from experiments shown in A and B.

References

1. L. Ting, R. Rad, S. P. Gygi, W. Haas, MS3 eliminates ratio distortion in isobaric multiplexed quantitative proteomics. *Nat Methods* 2011, *8*. 937-40, DOI: 10.1038/nmeth.1714

nmeth.1714 [pii].

2. J. Villen, S. P. Gygi, The SCX/IMAC enrichment approach for global phosphorylation analysis by mass spectrometry. *Nat Protoc* 2008, *3*. 1630-8, DOI: nprot.2008.150 [pii]

10.1038/nprot.2008.150.

3. D. Wessel, U. I. Flugge, A method for the quantitative recovery of protein in dilute solution in the presence of detergents and lipids. *Anal Biochem* 1984, *138*. 141-3, DOI: 0003-2697(84)90782-6 [pii].

4. E. L. Huttlin, M. P. Jedrychowski, J. E. Elias, T. Goswami, R. Rad, S. A. Beausoleil, J. Villen, W. Haas, M. E. Sowa, S. P. Gygi, A tissue-specific atlas of mouse protein phosphorylation and expression. *Cell* 2010, *143*. 1174-89, DOI: S0092-8674(10)01379-6 [pii]

10.1016/j.cell.2010.12.001.

5. J. K. Eng, A. L. McCormack, J. R. Yates, AN APPROACH TO CORRELATE TANDEM MASS-SPECTRAL DATA OF PEPTIDES WITH AMINO-ACID-SEQUENCES IN A PROTEIN DATABASE. *J. Am. Soc. Mass Spectrom.* 1994, *5*. 976-989, DOI: 10.1016/1044-0305(94)80016-2.

6. J. E. Elias, S. P. Gygi, Target-decoy search strategy for increased confidence in large-scale protein identifications by mass spectrometry. *Nat Methods* 2007, *4*. 207-14, DOI: nmeth1019 [pii]

10.1038/nmeth1019.

7. A. L. Rockwood, S. L. Vanorden, R. D. Smith, RAPID CALCULATION OF ISOTOPE DISTRIBUTIONS. *Analytical Chemistry* 1995, *67*. 2699-2704, DOI: 10.1021/ac00111a031.

8. Z. Q. Zhang, S. H. Guan, A. G. Marshall, Enhancement of the effective resolution of mass spectra of high-mass biomolecules by maximum entropy-based deconvolution to eliminate the isotopic natural abundance distribution. *J. Am. Soc. Mass Spectrom.* 1997, *8*. 659-670, DOI: 10.1016/s1044-0305(97)82982-0.

9. A. Makarov, E. Denisov, Dynamics of Ions of Intact Proteins in the Orbitrap Mass Analyzer. *J. Am. Soc. Mass Spectrom.* 2009, *20*. 1486-1495, DOI: 10.1016/j.jasms.2009.03.024.
10. A. Michalski, E. Damoc, O. Lange, E. Denisov, D. Nolting, M. Muller, R. Viner, J. Schwartz, P. Remes, M. Belford, J. J. Dunyach, J. Cox, S. Horning, M. Mann, A. Makarov, Ultra High Resolution Linear Ion Trap Orbitrap Mass Spectrometer (Orbitrap Elite) Facilitates Top Down LC MS/MS and Versatile Peptide Fragmentation Modes. *Mol Cell Proteomics* 2012, *11*. O111 013698, DOI: O111.013698 [pii]

10.1074/mcp.O111.013698.